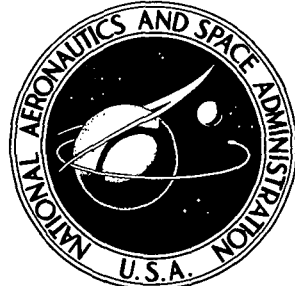


NASA CR-2235

NASA CONTRACTOR
REPORT



N73- 20936
NASA CR-2235

CAO/L FILE
COPY

SL4 CODE - A USER'S MANUAL

by Y. S. Chou

Prepared by

LOCKHEED MISSILES & SPACE COMPANY

Sunnyvale, Calif.

for Ames Research Center

NATIONAL AERONAUTICS AND SPACE ADMINISTRATION • WASHINGTON, D. C. • MARCH 1973

Page Intentionally Left Blank

1. Report No. NASA CR 2235	2. Government Accession No.	3. Recipient's Catalog No.	
4. Title and Subtitle SL4 Code--A User's Manual		5. Report Date March 1973	
		6. Performing Organization Code	
7. Author(s) Y.S. Chou		8. Performing Organization Report No.	
9. Performing Organization Name and Address Lockheed Missiles & Space Company Sunnyvale, California		10. Work Unit No.	
		11. Contract or Grant No. NAS 2-6668	
12. Sponsoring Agency Name and Address National Aeronautics & Space Administration Washington, D.C.		13. Type of Report and Period Covered Contractor Report	
		14. Sponsoring Agency Code	
15. Supplementary Notes			
16. Abstract The SL-4 code is a computer automated scheme for solving the equations describing the fully-coupled viscous, radiating flow over the front face of a blunt body which may or may not be ablating. The code provides a basis for obtaining predictions of the surface heating to a body entering any planetary atmosphere at hyperbolic velocities. The code is written in Fortran V and is operational on both the UNIVAC 1108 (EXEC 8) system in use at LMSC and the CDC 7600 system in use at the University of California, Berkeley. This report gives an overview of the SL-4 code computational logic flow, a description of the input requirements and output results and comments on the practical use of the code. As such this report forms a "users manual" for operation of the SL-4 code.			
17. Key Words (Suggested by Author(s)) Viscous, Radiation, Heating, Entry, Hypersonic, Planetary, Ablation, Boundary Layer		18. Distribution Statement UNCLASSIFIED - UNLIMITED	
19. Security Classif. (of this report) UNCLASSIFIED	20. Security Classif. (of this page) UNCLASSIFIED	21. No. of Pages 29	22. Price* \$3.00

* For sale by the National Technical Information Service, Springfield, Virginia 22151

Page Intentionally Left Blank

1. INTRODUCTION

The Lockheed Missiles and Space Company's SL4 Code is a computer implemented computational scheme which provides theoretical predictions of the radiative and convective energy transfer to the surface of a blunt body during hyper-velocity entry into planetary atmospheres. Although prediction of the convective heating rate is a direct consequence of the solution method, the SL4 Code was developed primarily to analyze those entry conditions where radiative processes dominate the total energy transport. The surface heating rate prediction results from a solution of the coupled equations describing the flow of a viscous, radiating gas past a blunt body which may or may not be undergoing massive ablation. The detailed derivation and analysis of those equations can be found in Ref. 1.

The solution provided by the SL4 Code is a solution to the inverse problem. In order to use this code, the shock wave must be specified completely. The body which supports this shock will be a part of the solution. In the SL4 Code, a specific shock equation was built-in. This equation contains two free parameters. Detailed discussion on this equation will be given in Section 3. It is believed that these two families of shock waves will be sufficient to describe many cases of practical interest.

The SL4 Code also requires an a priori specification of the streamwise variation of the surface blowing rate. A particular equation for the blowing rate distribution, which contains one free parameter, was built into the code. This equation will be discussed in Section 3. By performing an iterative process, the blowing rate distribution can be made to reflect the surface radiative flux.

Within the context of its application by a knowledgeable user, the code is operational on the UNIVAC 1108 (Exec. 8) system in use at IMSC and the CDC 7600 system in use at the University of California, Berkeley, California.

2. COMPUTATION STRUCTURE

A chart is given in Fig. 1 which shows the logic sequence followed in obtaining an iterative solution to the conservation equations. Details on the input/output quantities will be given in the next section. The first step in the SL4 Code computation is the determination of the shock layer parameters β 's. For the definitions of β 's, the reader should consult Ref. 1. The β 's are determined by the two separate subroutines. One subroutine supplies the shock shape and its derivatives, while the other subroutine describes the injection rate and computes the total injected mass and its derivatives. The next step in the computation is the determination of the properties behind the shock. From the oblique shock relations, the pressure and the tangential velocity are determined. After neglecting the normal velocity and the radiative energy loss right behind the shock, the enthalpy can be determined. A simple iteration using the FEMP subroutine to calculate the actual post shock density leads rapidly to a determination of all shock properties.

The sequential solution of the conservation equations is now initiated. The input estimates of the tangential velocity, blown gas mass fraction, total enthalpy, and their streamwise derivatives provide the data required to start the iteration process. The first step in the iterative cycle is to calculate collisional transport properties. This is accomplished using the FEMP package set of subroutines. Along with the enthalpy and elemental mass fractions (as deduced from the local value of the blown gas mass fraction), the FEMP routine requires a value for the pressure. This value is given by an analytic expression as presented in Ref. 1. From FEMP, the variation in temperature, density, viscosity and binary diffusion coefficient across the shock layer is obtained. These properties provide the data required to perform a solution to the momentum equations using the technique discussed in Ref. 1. Convergence of the velocity profile is obtained via a local iterative loop. For a fixed set of density and diffusion coefficient data together with the just-calculated velocity distribution,

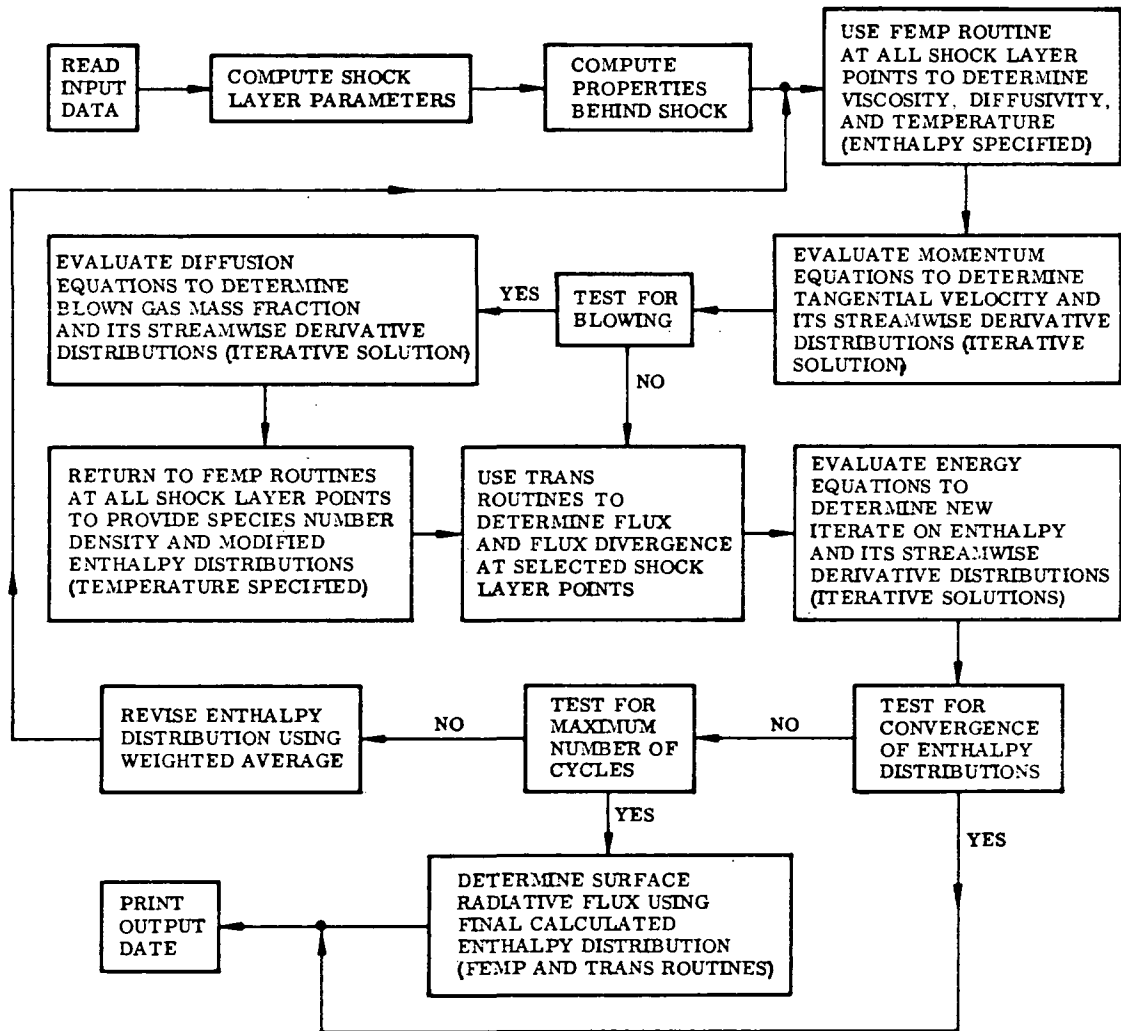


Fig. 1. Computational Logic Flow

the diffusion equation can be solved in a similar manner.

At this point our procedure elects to update the species number density distribution to reflect the change in the blown gas mass fraction profile. It is essential to recognize that in flows dominated by radiative transport effects, temperature is a crucial variable. Indeed, the temperature which is calculated in FEMP from the input enthalpy-mass fraction distribution must be a "reasonable" distribution. Having established a reasonable temperature distribution from the initial guess it is imperative to the stability of the solution to prevent the initial temperature profile from being altered to a large degree in a single step. Such a large temperature change often will occur if we hold the enthalpy at its initial value and calculate a new temperature, density and species number density profile using the updated elemental mass fraction distribution. The reason which underlies the temperature change problem is the following: For flows dominated by radiative transport and especially at high Reynolds numbers, the shear layer is nearly isothermal. However, a rapid change in elemental mass fraction occurs across the shear layer. Since the effective heat capacity of the blown gas may be quite different than that of the atmospheric gas, then the rapid change in the elemental mass fractions is accompanied by rapid change in the enthalpy despite the nearly isothermal character of the shear layer. Hence, if in the updating of the elemental mass fractions, the injected gas moves to a point where the enthalpy is significantly different, the resultant temperature is physically unrealistic and causes catastrophic failure of the energy equation.

To eliminate this high sensitivity between the diffusion and energy equations, our approach fixes temperature at the current value obtained on the first pass through FEMP. Thus in the second pass through FEMP, the temperature is the independent thermodynamic variable and updated values of enthalpy and species number density are determined. Of course, for a nonblowing there is no requirement for a second pass through FEMP. Thus, for a nonblowing problem, these two stages are bypassed as indicated in Fig. 1.

Having updated the species number densities and using the current

temperature profile, the next step is to determine the radiative flux divergence across the shock layer. In deriving the equations describing the radiative transport across the shock layer, it was convenient to use the physical shock layer normal coordinate. Accordingly, the first task in the radiative transport subroutine is to determine from the ω coordinate values and the density distribution the physical thickness of the shock layer. The radiative flux divergence is then calculated at every ω point. These flux divergence values are used along with the current velocity profile and Prandtl number variation to provide a new estimate for the enthalpy profile.

A test for convergence of the total enthalpy profile is made at this point in the computational cycle. Further comments on the level of convergence to be expected will be given in Section 4. If satisfactory convergence has not been achieved, the entire iterative procedure is reinitiated. A number of investigators besides the author have observed the instability which arises if the calculated enthalpy profile is used unaltered as the enthalpy profile for the subsequent iterative cycle. In the absence of a meaningful stability analysis (which is likely to be impossible to achieve in view of the strong nonlinearity of the radiative transport terms), the following expedient has been employed. Let H^i be the current guess on the enthalpy profile and H^{i+1} the resulting calculated value. Then the next guess on the enthalpy profile which will be used to reinitiate the iterative loop is

$$H_{\text{next}} = (1-m)H^i + mH^{i+1}$$

where m is a fraction less than 1.0. A practical upper limit on m appears to be 0.5. As $m \rightarrow 0$ stability will undoubtedly be achieved but at the cost of numerous iterations for significant progress toward convergence. Our experience has shown that $m \sim 0.2$ to 0.3 are reasonable values for blowing problems, while m may approach 0.5 for nonblowing.

If convergence is achieved or, as is more likely, a maximum number of iterative cycles have passed, then a final pass through the radiative transport subroutine is made. In this final pass the radiative flux at the wall is calculated using the unaltered enthalpy profile, $H = H^{i+1}$. This final wall

radiative flux value then can be compared against the value obtained from the enthalpy profile which existed upon the last entry to the energy equation. The comparison of these two flux values provides the best measure of convergence. Preparation of data for output, which is discussed in Section 3, completes the computation.

3. INPUT AND OUTPUT

3.1 Input Data

Table 1 lists the input data required to initiate a SL4 Code run. Also given in Table 1 is the data format, FORTRAN symbol and a synoptic description of each input quantity. The data is segregated into card groups. Depending on the amount of data required, more than one punched card may be needed in a given group. Figures 2 and 3 are copies from a computer listing of a set of input data. In the following discussion we shall proceed sequentially through Table 1. The reader will find it instructive to examine the typical values shown in Figs. 2 and 3 as we move through Table 1. The centimeter-gram-second system of units, along with °K for temperature, has been used for those input quantities given in dimensional form.

The data specified in the first card group is self-explanatory. The data specified in the second card group deals primarily with description of the free stream properties. Vehicle velocity and ambient density are self-explanatory. The shock bluntness β_s and the asymptotic shock angle θ_s are the two free parameters in describing the shock shape. In the SL4 Code, this shock shape is given by the following equation.

$$r_s^2 = 2z + r_s z \tan \theta_s - \beta_s z^2$$

Where z is the horizontal distance from shock stagnation point, and r_s is the normal distance from the axis of symmetry. For $\theta_s = 0$, this equation describes: a parabola if $\beta_s = 0$; a sphere if $\beta_s = 1$; a hyperbola if $\beta_s < 0$; and an ellipsoid if $\beta_s > 1$. For a nonzero value of θ_s , if $\beta_s = 0$, the shock shape equation describes a parabola near the nose and then asymptotically the shock shape approaches a cone with half angle equal to θ_s at large z .

The wall is characterized by either a prescribed enthalpy or (normally) temperature according to an option given in card group 6. If a prescribed wall enthalpy is input, that enthalpy must be normalized to the total free

stream enthalpy $h_\infty + u_\infty^2/2$. If a prescribed wall temperature is used, the value is input in dimensional ($^{\circ}\text{K}$) form.

The blowing rate is given in terms of a normalized value $\dot{m} = \rho_w v_w / \rho_\infty u_\infty$ which is given by the following equation as a function of r_s

$$\dot{m} = \frac{\dot{m}_o}{1 + Ar_s^2}$$

where \dot{m}_o is the blowing rate at stagnation point and the parameter A characterizes the rate change of the local blowing rate around the body.

The convergence criterion τ is applied by requiring

$$\frac{H^{i+1} - H^i}{(H^{i+1} + H^i)/2} < \tau$$

be satisfied at all shock layer points in order for convergence to be achieved. For nonblowing problems, convergence to a level of $\tau = .01$ (i.e., 1% convergence) is an achievable goal. However, for radiative dominated problems, a 1% convergence tolerance is probably too severe. Usually a few points in the shock layer hold up convergence. Hence, when a 1% convergence level is achieved the radiative flux at the wall is changing considerably less than 1% between iterations. A precision of 1% is inconsistent with the overall accuracy of the optical properties, transport properties and the assumption of chemical equilibrium which set the true error bound on the heating predictions. For blowing problems, convergence to a 5% level is rarely achieved. For blowing problems, convergence is much more reasonably measured by comparing the wall flux based on the final guessed and calculated enthalpy profile.

The weighting factor employed in stabilizing the successive iterations on the energy equation was discussed in the previous section.

The FEMP routine considers two different temperature ranges. These two ranges are denoted as the low temperature regime and the high temperature regime. The low temperature regime does not contain ionized species whereas the high temperature regime does not contain polyatomic species. A tabulation of the species considered in each temperature regime is given in Table I of

Table 1
SL4 Code Input Requirement

<u>Card Group</u>	<u>Format</u>	<u>Item</u>	<u>Description</u>
1	6A6	RUNID	Alphanumeric run identification
2	7E10.4	UIN RIN RS BS THS THW XMZ	Vehicle velocity (cm/sec) Ambient density (gm/cm ³) Shock radius of curvature at stagnation point Shock bluntness Asymptotic shock angle (deg) Wall enthalpy or wall temperature(°K) (see ICWT, card 6) Blowing rate at stagnation point
3	4E10.4	AAA CORR CONV TLH	Blowing rate parameter Weighting factor in enthalpy profile guess Convergence criteria enthalpy profile Low to high species temperature switch (°K)
4	5E10.4	ALPV(1) ALPV(2) ALPV(3) ALPV(4) ALPV(5)	Elemental mass fraction of H at wall Elemental mass fraction of He at wall Elemental mass fraction of C at wall Elemental mass fraction of N at wall Elemental mass fraction of O at wall
5	5E10.4	ALPA(1) ALPA(2) ALPA(3) ALPA(4) ALPA(5)	Elemental mass fraction of H at shock Elemental mass fraction of He at shock Elemental mass fraction of C at shock Elemental mass fraction of N at shock Elemental mass fraction of O at shock
6	7I5	NRS ITGS IDG ICWT MOL	Number of z points input (max. 10) Maximum number of iterations = 0 no diagnostic output; =1 diagnostic output = 0 h _v input; =1 T _w input = 0 without molecules; =1 with molecules

Table 1 (Continued)

<u>Card Group</u>	<u>Format</u>	<u>Item</u>	<u>Description</u>
6	7I5	LINES IRAD	= 0 without lines;=1 with lines = 0 no radiation;=1 with radiation
7	8E10.4	ZSS(I),I=1,NRS	z points
8	I5	NES	number of grid points input
9	8E10.4	w(K),K=1,NES	w grid points
10	8E10.4	SF(K),K=1,NES	Velocity profile guess
11	8E10.4	C(K),K=1,NES	Blown gas mass fraction profile guess (if XMZ=0, input C(K)=0)
12	8E10.4	H(K),K=1,NES	Enthalpy profile guess
13*	8E10.4	ETA(K),K=1,NES	Stream function guess
14*	8E10.4	CF(K),K=1,NES	F
15*	8E10.4	CX(K),K=1,NES	\bar{C}_v
16*	8E10.4	HX(K),K=1,NES	\bar{H}

* Input only if ZSS(1) > 10^{-4}

SL4 - VISCOUS RADIATING SHOCK LAYER WITH BLOWING VEHICLE AND FLIGHT CONDITIONS		TEST RUN
VEHICLE VELOCITY	= 4.0000+06 CM/SEC	
AMBIENT DENSITY	= 6.9000-07 GM/CM ³	
SHOCK RADIUS OF CURVATURE AT STAGNATION PT.	= 2.0000+01 CM	
WALL TEMPERATURE	= 4.5000+03 DEG,K	
SHOCK BLUNTNES	= 0.0000 NORMALIZED	
ASYMPTOTIC SHOCK ANGLE	= 6.2000+01 DEG,	
BLOWING RATE PARAMETER	= 1.0000-01	
BLOWING RATE AT STAGNATION PT.	= 4.0000-01 NORMALIZED	
LOCAL BLOWING RATE	= 3.4757-01 NORMALIZED	
LONGITUDINAL DISTANCE FROM SHOCK NOSE	= 3.5000-01 NORMALIZED	
 COMPOSITION BY ELEMENTAL MASS FRACTION		
ATMOSPHERE	HEAT SHIELD	
HYDROGEN	.740	.000
HELIUM	.260	.000
CARBON	.000	1.000
NITROGEN	.000	.000
OXYGEN	.000	.000
 PROGRAM OPTIONS AND PARAMETERS		
5.0 PERCENT CONVERGENCE ON ENERGY EQUATION		
15 WEIGHTING FACTOR IN ENTHALPY PROFILE SPECIFICATION		
700C LOW TO HIGH TEMPERATURE SPECIES SWITCH (DEG,K)		
21 SHOCK LAYER POINTS INPUT		
1 MAXIMUM ITERATIONS		
COUPLED RADIATIVE TRANSPORT		
MOLECULAR ABSORPTION INCLUDED IN RADIATIVE TRANSPORT		
ATOMIC LINES INCLUDED IN RADIATIVE TRANSPORT		
WALL TEMPERATURE SPECIFIED		
DIAGNOSTIC DATA REQUESTED		

Fig. 2. Input Data, Vehicle and Atmospheric Parameters

INITIAL SHOCK LAYER PROFILES

W	ETA	SF	H	CV	F	HBAR	CVBAR
0.00000	-5.00000e-01	0.00000	-2.00000e-03	1.00000e+00	0.00000	0.00000	0.00000
1.00000e-02	-4.30000e-01	3.00000e-03	1.00000e-03	1.00000e-03	0.00000	1.29000e-03	0.00000
2.00000e-02	-4.20000e-01	7.00000e-03	1.10000e-02	1.00000e-02	0.00000	3.20000e-03	0.00000
3.00000e-01	-4.10000e-01	1.10000e-02	3.00000e-02	1.00000e-02	0.00000	7.00000e-03	0.00000
4.00000e-01	-4.10000e-01	4.20000e-02	4.20000e-02	1.00000e-02	0.00000	1.00000e-02	0.00000
5.00000e-01	-3.60000e-01	2.40000e-02	4.90000e-02	1.00000e-02	0.00000	1.10000e-02	0.00000
6.00000e-01	-2.30000e-01	4.80000e-02	5.90000e-02	1.00000e-02	0.00000	9.00000e-03	0.00000
7.00000e-01	-1.60000e-01	7.50000e-02	6.00000e-02	1.00000e-02	0.00000	7.00000e-03	0.00000
8.00000e-01	-7.40000e-02	8.20000e-02	6.50000e-02	1.00000e-02	0.00000	6.00000e-03	0.00000
9.00000e-01	-1.30000e-02	1.00000e-01	9.00000e-02	9.70000e-02	0.00000	3.00000e-02	0.00000
4.00000e-01	1.00000e-02	4.90000e-01	7.00000e-01	0.00000	2.00000e-02	-2.00000e-02	7.00000e-02
4.10000e-01	3.90000e-02	6.60000e-01	7.50000e-01	0.00000	2.00000e-02	-5.00000e-02	0.00000
4.60000e-01	7.60000e-02	7.70000e-01	8.00000e-01	0.00000	1.10000e-01	-7.00000e-02	0.00000
5.60000e-01	1.50000e-01	8.20000e-01	8.60000e-01	0.00000	9.00000e-02	-3.4.00000e-02	0.00000
6.60000e-01	2.30000e-01	9.20000e-01	9.10000e-01	0.00000	6.00000e-02	-3.00000e-02	0.00000
7.60000e-01	3.10000e-01	9.50000e-01	9.40000e-01	0.00000	4.00000e-02	-2.00000e-02	0.00000
8.60000e-01	3.90000e-01	9.70000e-01	9.60000e-01	0.00000	2.00000e-02	-1.00000e-02	0.00000
9.50000e-01	4.60000e-01	9.80000e-01	9.80000e-01	0.00000	0.00000	0.00000	0.00000
9.90000e-01	4.90000e-01	9.90000e-01	9.90000e-01	0.00000	0.00000	0.00000	0.00000
1.00000e+00	5.10000e-01	1.00000e+00	1.00000e+00	0.00000	0.00000	0.00000	0.00000

Fig. 3. Input Data: Initial Shock Layer Profiles

Ref. 2. Changes to that tabulation since it was published include: (1) addition of C₃, He, H₂O and CO₂ to the low temperature regime; (2) addition of C₂, He and He⁺ to the high temperature regime. The SL4 code user must specify a temperature at which the FEMP calculation is switched from the low to high regimes. Selection of this low to high temperature break-point must take into consideration that it should be sufficiently high that polyatomic species would not be present in significant amounts (< 1%) at or above that temperature nor ionized species present in significant amounts at or below that temperature. The temperature break-point will depend on the stagnation-point pressure and typically will vary from 5000°K at low pressures (~ 0.1 atm) to 8000°K at high pressures (~ 100 atm). The solution is not critically dependent on the value of the break-point temperature selected. With a little experience in a given problem, an appropriate value for the temperature switch will be readily apparent to the user. An additional requirement is that the low to high temperature switch be greater than the wall temperature but less than the shock temperature.

The fourth and fifth card groups permit specification of an arbitrary ablation product (card group 4) and atmospheric (card group 5) gas composition. A fundamental restriction on the SL4 code is that the composition of ablator and atmosphere be comprised of H, He, C, N and O elements. The species included in the FEMP routine were selected on the basis of being the most significant for a mixture comprised of these elements.^{2,3} For both ablator or atmosphere the composition is given simply on an elemental mass fraction basis. The actual species composition of the gases entering the shock layer is not specified as this will be handled by FEMP.

The sixth card group provides control options. The number of shock layer points is at the discretion of the user. Storage limitations require that the number of shock layer points be kept equal to or less than 40. The maximum number of iterations provides a termination point for the calculation when "convergence" of the enthalpy profile is not achieved. On the UNIVAC 1108 Exec 8 system in operation at LMSC, the computation time for a full iterative cycle (i.e., solution of momentum, mass and energy equations including FEMP

and TRANS subroutines) for a typical problem involving 26 shock layer points is approximately 2 minutes. Computer time, then, is normally the overriding consideration in selection of the maximum number of iterations.

The remaining quantities in card group 6 are self-explanatory options. With regard to the diagnostic output, there will not be a discussion of the diagnostic data in Section 3.2. Without extensive study of the code details, the diagnostic data would have no utility to the user.

The last sequence of card groups specifies the computational grid (in the ω -coordinate) and initial estimates of the normalized distribution across the shock layer of the stream function η , tangential velocity f and its streamwise derivative F , the blowing gas mass fraction C_v and its streamwise derivative \bar{C}_v , the total enthalpy H and its streamwise derivative \bar{H} . Near the stagnation point ($z < 10^{-4}$) no estimates will be necessary for η , F , \bar{C}_v and \bar{H} . In the stagnation region F , \bar{C}_v and \bar{H} are zero. These estimates, of course, are crucial and a discussion of input profiles will be given in Section 4.

In addition to the normal input listed in Table 1, the user may also specify the spectral emissivity of the wall to account for surface emission and reflection. It was felt that it would be an inconvenience to require this spectral emissivity data to be input for every run. In a typical application of the SL4 code, we expect the surface properties to be fixed for a number of cases in which the atmospheric and vehicle parameters are varied. Accordingly, the spectral emissivity data are specified in an internally programmed data statement at the beginning of TRANS, the radiative transport subroutine. The data is specified in terms of the average emissivity within each of the 26 spectral groups employed in the continuum transport evaluation. That is to say, the SL4 code currently represents the spectral variation of surface emissivity by average values at 26 locations across the spectrum. The frequency values of the continuum groups are evident from the output discussed in the next subsection. For the line transport, the SL4 code lifts the surface emissivity values appropriate to the frequency interval of the various line groups in exactly the same way it determines the appropriate underlying continuum optical depth for

each line group. Currently, the SL4 code is programmed with unit surface emissivity for each continuum spectral interval.

3.2 Output Data

Figures 4 through 13 display copies of the computer listing of the output data for the problem defined by the set of input data shown in Figs. 2 and 3. In Fig. 4 the thermodynamic properties behind the normal shock are shown. In addition, the shock layer thickness, the normalized tangential velocity, the shock, body and the interface coordinate are output. Also included on Fig. 4 is a status report on the last energy equation iteration in terms of a comparison between the guessed and calculated enthalpy profile.

Figure 5 summarizes the radiative flux picture. Both the continuum and line fluxes (in W/cm^2) at the wall $Q + (0)$ and shock $Q - (1)$ are given as a function of the continuum and line group and, for convenience, the average spectral values (in $\text{W}/\text{cm}^2 \text{eV}$) in each group were output. The final quantity in Fig. 5 is the integral of the radiative flux divergence over the shock layer. This integral is to be compared with the sum of the continuum and line total fluxes (i.e., spectral summation) emergent from shock layer at the wall and shock. Agreement of the flux divergence integral with the total summation of all flux components demonstrates adequate spatial resolution of the flux divergence calculation across the shock layer.

The radiative flux is calculated at the same time the flux divergence is calculated. This allows us to present the radiative flux distribution across the shock layer in terms of the flux values at each ω -point. Figure 6 shows a representative set of radiative flux data. The ω coordinate and corresponding physical coordinate (normalized to total shock layer thickness) are indicated. This is followed by a listing of the continuum and line fluxes, in W/cm^2 , and the spectral summation. The spectral continuum optical depth evaluated at the midpoint of each continuum or line group is presented along with the flux values.

At the termination of the radiative flux output at the last shock layer point, $N = 1$, the wall convective and radiative heating values are presented. This is shown in Fig. 7. Of course, the radiative flux value was already output in terms of the continuum and line components in Fig. 5. These two radiative flux components are simply summed and repeated for convenience in the output indicated by Fig. 7. In addition to the absolute heating values, a convective and radiative heat transfer coefficient, defined as the heating rates normalized by $1/2 \rho_\infty u_\infty^3$, is presented as shown in Fig. 7.

A summary of the final values of the gasdynamic quantities--stream function, tangential velocity, enthalpy, ablation product mass fraction, flux divergence (W/cm^3) is output next. A representative set is shown as Fig. 8. A quick comparison between the initial and final profiles is thus available by examining the data of Figs. 3 and 8. It will be observed that the enthalpy tabulated in Fig. 8 is the weighted average of the final guessed and calculated values shown in Fig. 4. Thus this enthalpy profile represents the input to the next iteration. In principal, the output shown in Fig. 8 can be used directly to initiate a new set of iterations.

A summary of the thermodynamic and collisional transport properties consistent with the gasdynamic data given in Fig. 8 is the next data output. A representative set is shown as Fig. 9.

The next series of output presents the molecular and atomic species number density distributions across the shock layer. A representative set for the molecular species is shown as Fig. 10 and likewise for the atomic species as Fig. 11.

The final computation which the SL4 code performs is an evaluation of the radiative flux at the wall using the unaltered calculated enthalpy profile (as opposed to the profile weighted between guessed and calculated values) from the last iteration. The representative values of output which describes this final calculation is shown as Fig. 12. In Fig. 12, data from the FEMP routine is displayed with the temperature variable being of maximum interest.

The final output gives the continuum and line flux which may be compared with the data shown on Fig. 5 to assess the level of convergence of the overall radiative flux determination.

CONDITIONS BEHIND NORMAL SHOCK

PRESSURE = 9.8446e+00 ATMS
 ENTHALPY = 1.9229e+07 ERGS/GM
 TEMPERATURE = 1.6554e+04 DEG K
 DENSITY = 7.1811e-06 GM/CM³
 DENSITY JUMP = 9.6447e-02
 VISCOSITY = 5.9569e-04 CM/SEC
 REYNOLDS NUMBER = 9.2665e+04

SHOCK LAYER THICKNESS = 5.0151e+00 CM

NORMALIZED SHOCK COORDINATES Z_E = 3.5000e-01 R_E = 1.2292e+00NORMALIZED BODY COORDINATES Z_E = 5.8143e-01 R_E = 1.1366e+00NORMALIZED INTERFACE COORDINATES Z_E = 4.9738e-01 R_E = 1.1688e+00

LAST ENTHALFY PROFILE ITERATION

W	S _E	S _F	H(GUESS)	H(CALC)	C _V	F	H _{BAR}	CVBAR
0.00000	-5.00000e-01	3.72529e-09	-2.36173e-03	-2.36174e-03	1.00000e+00	0.06000	5.67175e-10	5.51662e-09
4.00000e-02	-4.92585e-01	3.02673e-03	6.19363e-04	1.01634e-03	1.00000e+00	-4.89632e-06	7.44395e-04	5.51662e-09
8.00000e-02	6.38615e-03	6.22640e-03	9.09690e-03	9.22640e-03	1.00000e+00	-2.14431e-05	2.5673e-03	5.51662e-09
1.20000e-01	-4.72662e-01	1.09690e-03	1.09690e-02	2.10179e-02	1.00000e+00	-5.63234e-05	5.68363e-03	5.51662e-09
1.60000e-01	-4.45486e-01	1.04596e-02	2.10179e-02	2.10179e-02	1.00000e+00	-1.24007e-04	8.80255e-03	5.51662e-09
2.00000e-01	-4.12381e-01	1.57231e-02	4.3761e-02	5.53136e-02	1.00000e+00	-2.42534e-04	9.96335e-03	5.51662e-09
2.40000e-01	-3.71368e-01	2.12364e-02	4.98547e-02	3.95292e-02	1.00000e+00	-6.98333e-04	1.02216e-02	5.16968e-09
2.80000e-01	-2.15544e-01	4.72505e-02	5.49514e-02	3.12950e-02	1.00000e+00	-8.00333e-04	1.05358e-02	5.03581e-07
3.20000e-01	-1.95333e-01	5.11213e-02	5.56436e-02	3.76163e-02	1.00000e+00	-1.00333e-03	1.0166e-02	5.03581e-07
3.60000e-01	-7.14457e-02	6.02641e-02	6.09928e-02	3.71379e-02	9.97975e-01	-1.73359e-03	8.6671e-03	3.16705e-03
4.00000e-01	-3.48324e-02	1.12029e-01	9.46968e-02	1.23948e-01	9.32997e-01	-1.44667e-03	-6.0619e-03	3.16738e-02
4.40000e-01	-3.10550e-02	2.31105e-01	2.49859e-01	4.67370e-01	5.11954e-01	-2.95249e-02	-2.9382e-02	1.72550e-02
4.80000e-01	-2.24556e-02	2.16174e-01	2.74337e-01	4.77435e-01	5.11549e-01	-3.07550e-02	-2.88109e-02	1.53623e-02
5.20000e-01	-6.64012e-01	2.18595e-01	2.12331e-01	5.64688e-01	3.39623e-01	-3.0854e-02	-3.32263e-02	5.33773e-04
5.60000e-01	2.43714e-02	2.24267e-01	6.16463e-01	8.12541e-01	-2.0894e-04	1.20032e-01	-6.6760e-02	1.37717e-03
6.00000e-01	4.39351e-02	6.19656e-01	7.06950e-01	6.54958e-01	-6.1281e-06	1.17972e-01	-7.0328e-02	3.59319e-05
6.40000e-01	8.20445e-02	7.43455e-01	7.19189e-01	8.3836e-01	3.2522e-09	1.07223e-01	-5.7530e-02	1.09162e-03
6.80000e-01	1.506561e-01	8.71783e-01	8.55161e-01	9.05902e-01	3.72529e-09	8.44460e-02	-4.0476e-02	2.70855e-10
7.20000e-01	2.35657e-01	9.21070e-01	9.02025e-01	9.30311e-01	3.72529e-09	6.2153e-02	-2.9526e-02	2.70855e-10
7.52500e-01	3.12166e-01	9.53234e-01	8.14869e-01	9.51887e-01	3.72529e-09	4.20761e-02	-2.0859e-02	2.70855e-10
8.52500e-01	3.58250e-01	9.66204e-01	9.59105e-01	9.6426e-01	3.72529e-09	2.134435e-02	-2.70855e-10	2.70855e-10
9.50000e-01	4.62491e-01	9.13026e-01	6.78180e-01	9.66607e-01	3.72529e-09	7.69979e-03	-6.17782e-03	-2.70855e-10
9.90000e-01	4.92572e-01	9.96682e-01	6.88466e-01	9.96503e-01	3.72529e-09	1.50246e-03	-1.61634e-03	-2.70855e-10
1.00000e+00	5.00000e-01	1.00000e+00	9.98695e-01	1.00000e+00	3.72529e-09	-7.81451e-10	3.39001e-10	-2.70855e-10

Fig. 4. Output Data: Shock Conditions and Status of Enthalpy Iteration

WALL AND SHOCK RADIATIVE FLUXES - SPECTRAL DISTRIBUTION

CONTINUUM CONTRIBUTION TO THE SPECTRAL FLUX

K	HNU	DHNU	Q+(0)	Q+/DHNU	Q-(1)	Q-/DHNU
1	.570	.500	8,774+02	1,755+03	1,115+03	2,230+03
2	1,230	.660	3,057+03	4,632+03	4,598+03	6,967+03
3	1,600	.370	2,590+03	7,006+03	3,567+03	9,648+03
4	2,000	.400	2,334+03	5,835+03	3,223+03	1,056+03
5	2,900	.901	4,781+02	5,313+02	7,215+03	8,216+03
6	3,200	.300	6,440+01	2,147+02	1,948+03	6,494+03
7	3,500	.300	2,569+03	8,563+03	4,984+03	1,661+04
8	4,000	.500	2,052+03	4,103+03	6,586+03	1,317+04
9	4,500	.500	9,631+02	1,926+03	4,646+03	9,292+03
10	5,000	.500	3,519+02	7,038+02	3,245+03	6,189+03
11	5,500	.500	8,160+02	1,632+03	2,192+03	4,385+03
12	6,000	.500	1,254+03	2,508+03	1,490+03	2,980+03
13	6,500	.500	8,891+02	1,778+03	1,020+03	2,040+03
14	7,000	.500	6,889+02	1,378+03	6,940+02	1,388+03
15	7,500	.500	3,104+02	6,209+02	4,766+02	9,532+02
16	8,000	.500	2,425+02	4,850+02	3,667+02	7,335+02
17	8,370	.370	4,191+03	1,133+02	2,016+02	5,448+02
18	9,000	.630	2,594+03	4,117+03	3,550+02	5,634+02
19	9,500	.500	2,673+01	5,347+01	1,734+02	3,469+02
20	9,790	.290	3,181+01	1,097+02	7,329+01	2,327+02
21	10,770	.980	7,888+02	8,049+02	3,675+02	3,750+02
22	11,050	.280	9,280+03	3,314+02	6,336+01	2,263+02
23	11,950	.900	7,911+06	8,790+06	1,508+02	1,676+02
24	13,400	1,450	1,179+06	8,128+07	9,903+01	6,830+01
25	14,330	.930	4,122+08	4,432+08	1,174+03	1,263+03
26	20,000	5,670	5,717+09	1,008+09	1,664+03	2,935+02
TOTAL FLUX		1,935+04		5,169+04		

LINE CONTRIBUTION TO THE SPECTRAL FLUX

J	HNUC	DHNU	Q+(0)	Q+/DHNU	Q-(1)	Q-/DHNU
1	1,300	.600	1,071+02	1,766+02	5,493+02	9,155+02
2	1,900	.600	3,161+03	5,263+03	4,692+03	7,021+03
3	2,700	.600	3,701+01	6,172+01	8,564+03	1,427+04
4	7,250	.500	-3,688+01	-7,377+01	3,673+02	7,345+02
5	8,050	.700	-2,801+05	-4,001+05	6,484+02	9,262+02
6	9,100	1,400	-5,352+01	-3,823+01	6,986+02	4,990+02
7	10,300	1,000	-3,668+03	-3,668+03	5,325+03	5,325+03
8	10,950	.300	-1,141+03	-3,805+03	1,076+01	3,585+01
9	11,550	.900	0,000	0,000	0,000	0,000
10	12,700	1,400	-2,615+10	-1,868+10	2,843+03	2,031+03
11	13,900	1,000	-2,194+12	-2,194+12	0,000	0,000
TOTAL FLUX		3,178+03		2,370+04		

TOTAL FLUX DIVERGENCE INTEGRATION = 9,5150+04

Figure 5

Output Data: Radiative Flux at Wall and Shock

SHOCK LAYER RADIATIVE TRANSPORT SUMMARY

-CONTINUUM CONTRIBUTION

GP	MNU1-HNU2	POS.FLUX	NEG.FLUX	OPT.DEP.	POS.FLUX	NEG.FLUX	OPT.DEP.	POS.FLUX	NEG.FLUX	OPT.DEP.	
1	0.0	8.774+02	2.109+02	0.000	8.774+02	2.109+02	1.416+08	8.774+02	2.109+02	2.795+07	
2	0.6	1.2	3.057+03	7.761+02	0.000	1.221+03	7.033+02	1.116+01	3.669+03	9.072+02	2.430+01
3	1.2	1.6	2.390+03	4.428+02	0.000	2.456+03	4.457+02	7.065+02	2.456+03	4.459+02	1.655+01
4	1.6	2.0	2.334+03	3.631+02	0.000	2.452+03	3.654+02	5.962+02	2.609+03	3.763+02	1.356+01
5	2.0	2.9	4.811+02	3.992+02	0.000	2.455+02	4.547+02	2.635+00	1.409+03	6.321+02	5.761+01
6	2.9	3.2	6.440+01	5.255+01	0.000	1.995+02	6.274+01	3.529+00	2.468+02	1.063+02	7.781+00
7	3.2	3.5	2.569+02	2.215+01	0.000	2.000+03	3.296+01	1.231+01	3.400+03	3.903+01	2.977+01
8	3.5	4.0	2.052+03	2.732+01	0.000	2.552+03	2.169+01	2.216+01	3.400+03	3.685+01	5.359+01
9	4.0	4.5	9.651+02	1.099+01	0.000	1.764+03	1.193+01	3.525+01	2.155+03	1.362+01	8.183+01
10	4.5	5.0	3.199+02	4.237+01	0.000	6.337+02	4.459+01	5.415+01	1.266+03	9.122+00	1.258+00
11	5.0	5.5	8.160+02	1.670+01	0.000	1.070+03	1.725+00	2.716+01	1.402+03	1.795+00	5.850+01
12	5.5	6.0	1.554+03	5.726+01	0.000	1.500+03	5.615+01	3.605+02	1.363+03	6.647+01	8.369+02
13	6.0	6.5	8.891+02	2.129+01	0.000	9.144+02	2.056+01	2.804+02	9.489+02	2.333+01	6.529+02
14	6.5	7.0	6.989+02	7.649+02	0.000	5.860+02	7.449+02	1.267+01	6.840+02	7.051+02	8.244+05
15	7.0	7.5	3.104+02	2.409+02	0.000	3.446+02	2.554+02	1.043+01	5.919+02	4.082+02	2.329+01
16	7.5	8.0	2.425+02	8.114+02	0.000	1.745+01	1.320+02	2.711+00	3.329+00	5.757+02	6.057+00
17	8.0	8.4	4.191+03	2.524+03	0.000	1.076+02	2.572+03	4.067+00	3.181+01	1.262+02	9.065+00
18	8.4	9.0	2.594+03	1.332+03	0.000	1.434+02	2.372+03	4.069+00	2.633+01	1.262+02	9.064+00
19	9.0	9.5	2.673+01	2.690+01	0.000	1.475+01	2.478+01	2.022+01	4.165+01	1.164+03	5.465+01
20	9.5	9.6	3.181+01	6.633+05	0.000	3.186+01	6.643+05	1.164+03	3.200+01	6.094+05	6.093+03
21	9.8	10.6	7.868+02	6.322+05	0.000	9.634+02	7.508+05	2.002+01	1.550+01	9.067+04	6.762+01
22	10.6	11.1	9.280+03	3.546+06	0.000	1.134+02	4.296+06	2.002+01	1.022+02	8.022+05	6.793+01
23	11.1	12.0	7.911+06	3.417+06	0.000	7.951+05	7.567+06	5.672+00	1.657+03	7.447+05	1.647+01
24	12.0	13.5	1.379+06	4.631+06	0.000	1.371+05	1.133+06	5.672+00	4.149+04	1.370+05	1.647+01
25	13.4	14.3	9.122+05	1.412+08	0.000	6.421+07	3.906+08	5.672+00	2.053+01	5.415+07	1.647+01
26	14.3	20.0	5.177+09	1.754+09	0.000	1.116+07	5.339+09	5.672+00	6.796+06	1.115+07	1.647+01
			1.935+14	2.324+03		2.206+04	2.404+03		2.697+04	2.756+03	

LINE-CONTINUATION

GP	MNU1-HNU2	POS.FLUX	NEG.FLUX	OPT.DEP.	POS.FLUX	NEG.FLUX	OPT.DEP.	POS.FLUX	NEG.FLUX	OPT.DEP.	
1	1.0	1.6	1.071+02	0.605	0.000	1.157+02	5.123+04	7.666+02	1.244+02	6.216+03	1.655+01
2	1.6	2.2	3.61+03	0.605	0.000	3.155+03	5.121+04	5.962+02	5.631+02	5.211+05	1.386+01
3	2.4	3.0	3.03+01	0.605	0.000	5.114+00	0.400	2.635+00	1.174+02	0.000	5.761+00
4	7.0	7.5	3.688+01	0.600	0.000	4.060+01	4.427+04	1.043+01	4.541+01	8.443+03	2.326+01
5	7.7	8.4	2.031+05	0.600	0.000	5.592+04	5.563+06	4.067+00	2.032+02	8.465+06	9.065+00
6	8.4	9.8	-5.352+01	0.600	0.000	6.952+01	2.904+05	2.622+01	9.624+01	2.563+04	8.865+01
7	9.8	10.6	-3.665+02	0.600	0.000	4.334+02	6.231+07	2.012+01	-6.445+03	5.753+06	6.793+01
8	10.6	11.1	-1.141+03	0.600	0.000	1.341+03	1.344+07	2.002+01	-1.968+03	1.429+06	6.798+01
9	11.1	12.0	0.000	0.600	0.000	0.000	0.000	5.672+00	0.000	1.647+01	1.647+01
10	12.0	13.4	-2.615+10	0.600	0.000	7.148+11	1.995+11	5.672+00	-5.952+14	2.136+12	1.647+01
11	13.4	14.4	-2.194+12	0.600	0.000	9.763+13	1.210+13	5.672+00	-1.319+15	2.120+14	1.647+01
			3.178+03	0.600		3.166+03	9.915+04		3.733+03	9.389+03	

Output Data: Typical Radiative Flux Data at Selected Shock Layer Points

Figure 6

1	0-	6	1.919+02	1.113+03	9.768+00	0.000	1.113+03	9.956+00
2	1-6	1-2	1.195+02	4.547+03	1.259+00	0.000	4.598+03	1.722+00
3	1-2	1-6	6.122+01	3.519+03	7.697+01	0.000	3.567+03	7.790+01
4	1-6	2-0	6.474+01	3.174+03	5.425+01	0.000	3.221+03	5.475+01
5	2-0	2-9	8.652+01	7.144+03	1.019+01	0.000	7.215+03	1.020+01
6	2-9	3-2	1.789+01	1.933+03	1.395+01	0.000	1.948+03	1.395+01
7	3-2	3-5	1.167+02	4.905+02	1.079+00	0.000	4.784+03	1.088+00
8	3-5	4-0	1.453+02	6.474+03	1.497+00	0.000	6.586+03	1.502+00
9	4-0	4-5	1.062+02	4.564+03	1.812+00	0.000	4.646+03	1.846+00
10	-4-5	5-0	5.905+01	3.188+03	2.111+00	0.000	3.245+03	2.433+00
11	5-0	5-5	4.751+01	2.149+03	1.120+00	0.000	2.192+03	1.102+00
12	5-5	6-0	3.266+01	1.466+03	2.589+00	0.000	1.720+03	2.545+01
13	6-0	6-5	2.244+01	9.986+02	1.999+01	0.000	1.944+02	2.012+01
14	6-5	7-0	1.241+01	6.793+02	5.660+02	0.000	6.947+02	5.759+02
15	7-0	7-5	1.354+01	4.664+02	4.680+01	0.000	4.762+02	4.698+01
16	7-5	8-0	7.263+00	3.597+02	1.154+01	0.000	3.667+02	1.110+01
17	8-0	8-4	3.671+00	1.970+02	1.633+01	0.000	2.016+02	1.632+01
18	8-4	9-0	4.532+00	3.504+02	1.762+01	0.000	3.557+02	1.762+01
19	9-0	9-5	2.355+00	1.712+02	2.179+00	0.000	1.734+02	2.176+00
20	9-5	9-8	1.011+00	7.231+01	1.115+00	0.000	7.329+01	1.116+00
21	9-8	10-8	2.154+00	3.655+02	3.028+01	0.000	3.075+02	3.029+01
22	10-6	11-1	3.760+01	5.201+01	3.028+01	0.000	6.336+01	3.028+01
23	11-1	12-0	7.758+01	1.501+02	2.490+02	0.000	1.504+02	2.446+02
24	12-0	13-4	5.275+01	9.852+01	2.990+02	0.000	9.903+01	2.490+02
25	13-4	14-3	8.807+02	1.132+03	3.679+02	0.000	3.674+03	3.621+02
26	14-3	20-0	1.250+03	1.604+03	3.679+02	0.030	1.564+03	3.693+02
			3.275+13	5.048+34		0.000	5.169+04	

LINE CONTINUATION

(W# 390 T-W#) = 9.996+01) (W# 1.000 1-Y/D = 1.000+00)

(W# 1.000 1-Y/D = 1.000+00)

GP	HNU1-HNU2	SOS.FLUX	NEG.FLUX	OPT.DEP.	SOS.FLUX	NEG.FLUX	OPT.DEP.	PoS.FLUX	NEG.FLUX	OPT.DEP.
1	1-0	1-6	1.334+02	5.544+02	7.697+01	0.000	5.493+02	7.790+01		
2	1-6	2-2	6.375+02	4.663+03	5.125+01	0.000	4.592+03	5.475+01		
3	2-4	3-0	5.157+02	8.472+03	1.019+01	0.000	8.364+03	1.020+01		
4	3-0	7-5	3.011+01	3.476+02	4.690+01	0.000	3.673+02	4.698+01		
5	7-5	8-4	0.000	5.467+02	1.653+01	0.000	6.484+02	1.653+01		
6	8-4	9-8	0.000	6.962+02	2.176+00	0.000	6.986+02	2.176+00		
7	9-8	10-8	1.826+03	5.241+03	3.028+01	0.000	5.125+03	3.028+01		
8	10-8	11-1	3.070	1.576+01	3.028+01	0.000	1.576+01	3.028+01		
9	11-1	12-0	3.070	3.000	2.190+02	0.000	0.100	2.190+02		
10	12-0	13-4	1.133+03	2.767+03	2.190+02	0.000	2.143+03	2.490+02		
11	13-4	14-4	0.000	0.000	3.679+02	0.000	0.360	3.693+02		
			4.612+03	2.342+04		0.000	2.370+04			

HEAT TRANSFER VALUES

CONVECTIVE FLUX = 1.0045+01 W/CM2
 CONVECTIVE FLUX COEFFICIENT = 4.5042+06
 SURFACE RADIATIVE FLUX = 2.2532+04 W/CM2
 SURFACE RADIATIVE FLUX COEFFICIENT = 1.0262+02

Figure 7

Output Data: Convective and Radiative Fluxes

SHOCK LAYER GASDYNAMIC SUMMARY

	W	Y/D	ETA	SF	H	CV	G
0.00000	1.00000+00	5.00000-01	5.72529-09	*2.31173-03	1.00000+00	7.46749-02	
4.00000-02	9.73198-01	*4.92585-01	3.02673-03	1.01193-03	1.00000+00	2.35538-01	
3.00000-02	2.44447-01	*4.72662-01	6.38615-03	1.07071-02	1.00000+00	4.51278-01	
1.20000-01	9.11593-01	-4.45445-01	1.04596-02	2.08397-02	1.00000+00	5.40736-01	
1.60000-01	8.72114-01	-4.12381-01	1.57231-02	4.10112-02	1.00000+00	2.00632-01	
2.00000-01	8.28692-01	-3.71380-01	2.23647-02	4.75419-02	1.00000+00	2.65666-02	
3.00000-01	7.20143-01	-2.15648-01	4.75055-02	5.24510-02	1.00000+00	-4.56381-03	
3.10000-01	7.19152-01	-1.95333-01	5.11314-02	5.31030-02	1.00000+00	-1.39503-02	
4.69242-01	6.57164-01	-7.14857-02	8.02641-02	5.61120-02	9.97975-01	-2.86374-02	
5.72500-01	5.65153-01	-3.43524-02	1.12029-01	9.1861-02	9.32997-01	-2.63739-01	
5.82500-01	6.56297-01	-3.10550-03	2.31156-01	2.02440-01	5.5194-01	-1.82655-02	
5.82756-01	5.56180-01	=2.24556-03	2.36174-01	2.81226-01	5.14549-01	2.66913-01	
5.84912-01	6.34101-01	2.24262-03	2.85895-01	3.151215-01	3.39623-01	3.17349-01	
5.92500-01	6.17164-01	2.35014-02	6.16483-01	5.75411-01	-2.09894-04	1.69732-01	
6.02500-01	6.12168-01	4.39350-02	6.94656-01	7.22151-01	-6.17281-06	-1.67986-01	
6.52500-01	5.45302-01	6.20845-02	7.83455-01	8.04119-01	3.72529-09	-2.49500-01	
5.52500-01	4.39261-01	1.38561-01	8.71763-01	8.62773-01	3.72529-09	-2.72132-01	
6.52500-01	3.37450-01	2.32659-01	9.21070-01	9.06978-01	3.72529-09	-3.13482-01	
7.52500-01	2.37201-01	3.12166-01	9.53234-01	9.37319-01	3.72529-09	-3.50272-01	
3.52500-01	1.40617-01	3.88469-01	9.76220-01	9.51038-01	3.72529-09	-3.93415-01	
2.52500-01	4.72199-02	4.82491-02	9.93026-01	9.71318-01	3.72529-09	-5.14458-01	
3.90000-01	9.37462-03	4.92572-01	9.98682-01	9.89671-01	3.72529-09	-1.13482-00	
1.00000+00	0.000500	5.000000-01	1.000000+00	9.93891-01	3.72529-09	-1.28991+00	

Figure 8

Output Data: Shock Layer Gasdynamic Variables

SHOCK LAYER THERMODYNAMIC AND TRANSPORT SUMMARY

W	Y/D	(ERGS/GM)	(GM/GM3)	(GM/GM-SEC)	MU (GM2/GM4- SEC)	RM, (GM2/GM4- SEC)	T (DEG.K)	PR (ERGS/GM- DEG.K)	CPB (ERGS/GM- DEG.K)	K5 (ERGS/CM- SEC -DEG.K)
.0050	1.0000+00	-1.4694+10	6.6141+04	1.2389+23	8.1945+07	4.5000+03	4.5102+01	1.1537+08	3.1695+05	
.0450	9.7320+01	5.3043+09	5.9137+04	1.2950+03	7.5289+07	4.7013+03	4.7605+01	1.5396+08	4.1630+05	
.0910	9.445+01	5.3043+09	4.2232+03	1.2950+03	6.0167+07	5.1489+03	5.1937+01	2.2113+08	5.4313+05	
.1200	9.1169+01	2.1170+13	2.5747+04	1.6734+03	4.3067+07	5.8746+03	6.4727+01	1.6956+08	2.3407+05	
.1600	8.7221+01	5.3499+11	1.6071+04	1.9929+03	3.6014+07	5.9354+03	1.0312+03	5.3260+07	1.1291+05	
.2000	8.2670+01	5.7975+11	1.4806+04	2.0930+03	3.6975+07	4.0956+03	9.7656+01	3.1604+07	6.7912+04	
.2500	7.2034+01	4.1693+11	1.2492+04	2.0502+03	2.5612+07	9.4032+03	9.7083+01	3.5989+07	7.4555+04	
.3100	7.0535+01	4.2176+11	1.2245+04	2.0502+03	2.4864+07	9.5611+03	9.6295+01	7.7411+07	7.436+04	
.3600	6.5706+01	4.4526+11	1.1305+04	1.9244+03	2.1756+07	1.0224+04	9.9209+01	4.4597+07	8.501+04	
.3725	6.4505+01	2.7782+11	9.4399+05	1.796+03	1.6224+07	1.3134+04	9.2582+01	6.0049+07	1.1066+05	
.3925	6.3630+01	2.1961+12	5.5152+05	1.616+03	6.3135+06	1.0085+04	7.5217+01	7.3601+07	1.6733+05	
.3628	6.3606+01	2.3394+12	5.6913+05	1.6359+05	9.1394+06	1.0010+04	7.4120+01	7.4120+01	1.7026+05	
.3940	6.3110+01	2.7048+12	5.1945+05	1.6256+03	8.4443+06	1.0415+04	6.8694+01	7.7529+07	1.9368+05	
.3925	6.1706+01	2.1635+12	2.1495+05	1.1930+03	2.4159+05	1.1461+04	8.5139+01	2.7729+08		
.4025	6.0267+01	2.2639+12	8.3349+06	6.3921+04	6.9360+09	1.3734+04	1.6516+03	6.5946+08	3.3222+05	
.4525	5.4516+01	3.7035+12	7.7059+06	7.6657+04	5.9841+09	1.4337+04	1.7762+09	7.6229+08	3.2942+05	
.5525	4.3926+01	6.3098+12	7.5036+06	7.3337+04	5.5229+09	1.4680+04	1.8380+00	8.2163+08	3.2778+05	
.6525	3.3105+01	6.2497+12	7.2941+06	7.0673+04	5.1266+09	1.4946+04	1.8780+00	8.6756+08	3.2641+05	
.7525	2.3756+01	6.1228+12	7.1711+06	6.9224+04	4.8456+09	1.5110+04	1.9606+00	8.9645+08	3.2549+05	
.8525	1.4002+01	6.5344+12	7.1059+06	6.8443+04	4.8356+09	1.5225+04	1.9134+00	9.1385+08	3.2492+05	
.9520	4.7220+02	6.6565+12	7.0265+06	6.6244+04	4.7024+09	1.5347+04	1.9270+00	9.3346+08	3.2420+05	
.9630	9.3368+02	6.7344+12	6.9853+06	6.6374+04	4.6364+09	1.5407+04	1.9333+00	9.4342+08	3.2383+05	
1.0000	0.0000	6.1551+12	6.9300+06	6.5744+04	4.5558+09	1.5473+04	1.9401+00	9.5453+08	3.2338+05	

Figure 9

Output Data: Shock Layer Thermodynamic and Transport Variables

SHOCK LAYER CHEMICAL SPECIES SUMMARY

MOLECULAR SPECIES (PARTICLES/cm³)

W	V/D	C2+	C3H	C4H	HCN	C2H2	C3	C2	H2	N2	O2	CO	CN
0.00	1.00±0.00	0.00	0.00	0.00	0.00	8.20±16	3.54±18	0.00	0.00	0.00	0.00	0.00	0.00
4.00±02	9.73±01	0.10	0.00	0.00	0.00	6.14±18	4.22±18	0.00	0.00	0.00	0.00	0.00	0.00
6.00±02	9.44±01	0.10	0.00	0.00	0.00	2.47±18	4.71±18	0.00	0.00	0.00	0.00	0.00	0.00
1.20±01	9.42±01	0.40	0.60	0.00	0.00	2.12±17	2.35±18	0.00	0.00	0.00	0.00	0.00	0.00
1.60±01	8.73±01	0.40	0.00	0.00	0.00	3.79±15	4.60±17	0.00	0.00	0.00	0.00	0.00	0.00
2.00±01	8.30±01	0.40	0.00	0.00	0.00	9.35±16	0.00	0.00	0.00	0.00	0.00	0.00	0.00
3.00±01	7.20±01	0.40	0.00	0.00	0.00	2.33±16	0.00	0.00	0.00	0.00	0.00	0.00	0.00
3.00±01	7.03±01	0.10	0.00	0.00	0.00	2.00±16	0.00	0.00	0.00	0.00	0.00	0.00	0.00
3.00±01	6.97±01	0.30	0.00	0.00	0.00	1.11±16	0.00	0.00	0.00	0.00	0.00	0.00	0.00
3.12±01	6.45±01	0.00	0.00	0.00	0.00	2.68±15	0.00	0.30	0.00	0.00	0.00	0.00	0.00
3.02±01	6.36±01	0.30	0.00	0.00	0.00	3.00	1.61±14	0.00	0.00	0.00	0.00	0.00	0.00
3.03±01	6.34±01	0.00	0.00	0.00	0.00	1.70±14	0.00	0.00	0.00	0.00	0.00	0.00	0.00
3.08±01	6.34±01	0.00	0.00	0.00	0.00	6.90±13	0.00	2.00	0.00	0.00	0.00	0.00	0.00
3.92±01	6.17±01	0.00	0.00	0.00	0.00	0.00	0.00	0.00	0.00	0.00	0.00	0.00	0.00
4.02±01	6.03±01	0.00	0.00	0.00	0.00	0.00	0.00	0.00	0.00	0.00	0.00	0.00	0.00
4.62±01	5.44±01	0.30	0.00	0.00	0.00	0.00	0.00	0.00	0.00	0.00	0.00	0.00	0.00
5.52±01	4.39±01	0.00	0.00	0.00	0.00	0.00	0.00	0.00	0.00	0.00	0.00	0.00	0.00
6.52±01	3.37±01	0.00	0.00	0.00	0.00	0.00	0.00	0.00	0.00	0.00	0.00	0.00	0.00
7.52±01	2.31±01	0.00	0.00	0.00	0.00	0.00	0.00	0.00	0.00	0.00	0.00	0.00	0.00
8.52±01	1.41±01	0.00	0.00	0.00	0.00	0.00	0.00	0.00	0.00	0.00	0.00	0.00	0.00
9.50±01	4.72±02	0.30	0.00	0.00	0.00	0.00	0.00	0.00	0.00	0.00	0.00	0.00	0.00
9.90±01	9.38±03	0.00	0.00	0.00	0.00	0.00	0.00	0.00	0.00	0.00	0.00	0.00	0.00
1.00±00	0.00	0.00	0.00	0.00	0.00	0.00	0.00	0.00	0.00	0.00	0.00	0.00	0.00

Figure 10

Output Data: Shock Layer Polyatomic and Diatomic Species

SHOCK LAYER CHEMICAL SPECIES SUMMARY

ATOMIC SPECIES (PARTICLES/CM³)

	W	Y/D	H	C	N	O	HE	H+	C+	N+	C+	HE+	H-	E-
	0.00	1.00+00	0.00	1.49+16	0.00	0.00	0.00	0.00	0.00	0.00	0.00	0.00	0.00	0.00
4.00+02	7.73+01	0.00	2.31+18	0.00	0.00	0.00	0.00	0.00	0.00	0.00	0.00	0.00	0.00	0.00
8.00+02	9.44+01	0.30	4.39+18	0.00	0.00	0.00	0.00	0.00	0.00	0.00	0.00	0.00	0.00	0.00
1.20+01	9.12+01	0.00	7.50+18	0.00	0.00	0.00	0.00	0.00	0.00	0.00	0.00	0.00	0.00	0.00
1.60+01	8.73+01	0.30	8.13+16	0.00	0.00	0.00	0.00	0.00	0.00	0.00	0.00	0.00	0.00	0.00
2.00+01	8.30+01	0.30	7.20+18	0.00	0.00	0.00	0.00	0.00	0.00	0.00	0.00	0.00	0.00	0.00
3.00+01	7.20+01	0.30	6.10+18	0.00	0.00	0.00	0.00	1.20+17	0.00	0.00	0.00	0.00	0.00	1.20+17
3.10+01	7.09+01	0.06+11	5.97+18	0.00	0.00	7.14+10	9.67+08	1.35+17	0.00	0.00	5.02+02	3.60+07	1.35+17	
3.40+01	6.57+01	1.00+17	5.43+18	0.00	0.00	8.16+15	2.59+14	2.08+17	0.00	0.00	3.05+08	6.31+12	2.08+17	
3.72+01	6.45+01	2.79+18	4.07+18	0.00	0.00	2.49+17	2.21+16	3.69+17	0.00	0.00	7.148+10	1.96+14	3.90+17	
3.82+01	6.36+01	1.10+19	3.66+18	0.00	0.00	1.07+18	1.41+17	1.97+17	0.00	0.00	4.06+14	3.38+17		
3.83+01	6.36+01	1.21+19	1.29+18	0.00	0.00	1.98+18	1.36+17	1.82+17	0.00	0.00	3.79+11	3.93+14	3.18+17	
3.84+01	6.34+01	1.30+19	7.84+17	0.00	0.00	1.34+18	1.39+17	1.91+17	0.00	0.00	3.29+11	3.93+14	3.18+17	
3.92+01	6.17+01	6.67+18	0.00	0.00	7.89+17	2.33+17	0.00	0.00	0.00	0.00	2.112+11	3.18+14	2.39+17	
4.02+01	6.03+01	3.32+16	0.00	0.00	1.26+17	3.67+17	0.00	0.00	0.00	0.00	1.123+12	2.67+14	2.33+17	
4.52+01	5.46+01	2.39+18	0.00	0.00	2.05+17	4.15+17	0.00	0.00	0.00	0.00	1.234+13	2.12+14	3.67+17	
5.52+01	4.39+01	2.31+16	0.00	0.00	2.94+17	5.07+17	0.00	0.00	0.00	0.00	2.35+13	2.15+14	4.52+17	
6.52+01	3.37+01	2.68+18	0.00	0.00	2.86+17	5.53+17	0.00	0.00	0.00	0.00	2.14+14	5.09+17		
7.52+01	2.38+01	2.52+18	0.00	0.00	2.81+17	5.82+17	0.00	0.00	0.00	0.00	4.36+13	2.12+14	5.53+17	
8.52+01	1.41+01	2.54+18	0.00	0.00	2.78+17	6.00+17	0.00	0.00	0.00	0.00	5.14+13	2.10+14	5.81+17	
9.50+01	4.72+02	2.49+16	0.00	0.00	2.75+17	6.21+17	0.00	0.00	0.00	0.00	6.39+13	2.08+14	6.00+17	
9.90+01	9.36+03	2.46+18	0.00	0.00	2.73+17	6.32+17	0.00	0.00	0.00	0.00	6.76+13	2.06+14	6.32+17	
1.03+00	0.00	2.42+18	0.00	0.00	2.71+17	6.43+17	0.00	0.00	0.00	0.00	7.18+13	2.03+14	6.42+17	

Figure 11

Output Data: Shock Layer Atomic Species

FLUX USING LAST CALCULATED ENTHALPY PROFILE

R	P	T	X¹U	PR	D12	RHX	PR/
0.00000	7.44101701	4.56000+02	9.58669+02	2.07963+00	6.51017+01	-5.33013+01	51.19858+02
-4.00000-02	7.44103+01	4.56242+03	9.58661+02	2.17439+C0	6.7604+01	-4.71595+01	51.10543+02
6.00000-02	7.44105+01	4.56448+03	9.58656+02	2.15450+09	5.5215+01	-3.65941+01	8.616C6+01
1.20010-01	7.44105+01	5.56168+03	4.422492+02	2.64002+03	7.44600+01	-2.54248+01	36.71220+01
1.60005-01	7.45113+01	6.17616+03	3.26192+02	2.97545+03	9.5543+01	-1.39021+01	5.2423+01
2.00010-01	7.45113+01	6.40000+03	2.93745+02	3.15553+03	9.9750+01	-1.71377+01	5.3357+01
3.00005-01	7.48135+01	6.37834+03	3.01331+02	3.08419+03	9.42688+01	-2.88K66+01	55.55733+01
3.10000-01	7.48137+01	6.35050+03	3.11008+02	3.05560+03	9.69277+01	-2.84198+01	5.63151+01
3.60000-01	7.50031+01	5.8973+03	3.66573+02	2.81507+03	8.61975+01	-2.55732+01	56.14214+01
3.72000-01	7.5053+01	7.2555+03	2.75125+01	1.98042+04	2.4052+01	-4.27372+00	-6.5374+00
3.82500-01	7.5077+01	7.53589+04	1.58665+01	1.21106+04	1.29163+00	-1.06332+00	3.34446+00
3.82776-01	7.5077+01	7.53664+04	1.58664+01	1.21106+04	1.31194+00	-1.05731+00	51.1214+00
3.84007-01	7.5104+01	7.53664+04	1.49510+01	1.25596+00	1.00141+00	-1.02751+00	51.11019+00
3.92200-01	7.52272+01	1.52621+04	1.32667+01	1.13954+00	1.21309+10	-1.05732+00	-6.75994+01
4.02545-01	7.52553+01	1.49626+04	1.30511+01	1.18304+00	1.9612+00	1.03165+00	-6.12351+01
4.52200-01	7.54034+01	1.46392+04	1.04123+01	1.81149+00	1.48113+00	1.02942+00	-6.20341+01
5.52500-01	7.56345+01	1.41229+04	1.041229+01	1.69165+00	1.91615+00	1.03390+00	-6.28843+01
6.52400-01	7.5975+01	1.52291+04	1.15314+01	1.5557+00	1.0259+00	1.03390+00	-6.36562+01
7.52200-01	7.6257+01	1.22166+04	1.005702+01	1.14227+00	1.91293+00	-1.04422+00	-4.43983+01
8.52200-01	7.6551+01	1.25119+04	1.03021+01	1.2953+01	1.9241+03	1.00909+00	-6.513552+01
9.50000-01	7.6674+01	1.53505+04	1.01284+01	1.16132+00	1.93176+00	1.05442+00	-6.7877+01
9.90000-01	7.6935+01	1.24612+04	1.020669+01	1.106696+00	1.93798+00	1.05914+00	-6.58567+01
1.00000+00	7.69394+01	1.54712+04	1.003235+01	1.103604+00	1.94013+00	-6.58230+01	-7.26422+01

DELTA= 4.6661717+00 CH

CONTINUUM FLUX = 1.6629+34
LINE FLUX = 3.3316+01

PR/ = 51.19858+02

RHX = -5.33013+01

R¹X = 5.63151+01

R¹H = -6.75994+01

R¹P = -6.12351+01

R¹R = -6.28843+01

R¹V = -6.36562+01

R¹W = -6.35521+01

R¹Z = -6.20341+01

R¹A = -6.2325+01

R¹B = -6.32925+01

R¹C = -6.32925+01

R¹D = -6.32925+01

R¹E = -6.32925+01

R¹F = -6.32925+01

R¹G = -6.32925+01

R¹H = -6.32925+01

R¹I = -6.32925+01

R¹J = -6.32925+01

R¹K = -6.32925+01

R¹L = -6.32925+01

R¹M = -6.32925+01

R¹N = -6.32925+01

R¹O = -6.32925+01

R¹P = -6.32925+01

R¹Q = -6.32925+01

R¹R = -6.32925+01

R¹S = -6.32925+01

R¹T = -6.32925+01

R¹U = -6.32925+01

R¹V = -6.32925+01

R¹W = -6.32925+01

R¹Z = -6.32925+01

R¹A = -6.32925+01

R¹B = -6.32925+01

R¹C = -6.32925+01

R¹D = -6.32925+01

R¹E = -6.32925+01

R¹F = -6.32925+01

R¹G = -6.32925+01

R¹H = -6.32925+01

R¹I = -6.32925+01

R¹J = -6.32925+01

R¹K = -6.32925+01

R¹L = -6.32925+01

R¹M = -6.32925+01

R¹N = -6.32925+01

R¹P = -6.32925+01

R¹Q = -6.32925+01

R¹R = -6.32925+01

R¹S = -6.32925+01

R¹T = -6.32925+01

R¹U = -6.32925+01

R¹V = -6.32925+01

R¹W = -6.32925+01

R¹Z = -6.32925+01

R¹A = -6.32925+01

R¹B = -6.32925+01

R¹C = -6.32925+01

R¹D = -6.32925+01

R¹E = -6.32925+01

R¹F = -6.32925+01

R¹G = -6.32925+01

R¹H = -6.32925+01

R¹I = -6.32925+01

R¹J = -6.32925+01

R¹K = -6.32925+01

R¹L = -6.32925+01

R¹M = -6.32925+01

R¹N = -6.32925+01

R¹P = -6.32925+01

R¹Q = -6.32925+01

R¹R = -6.32925+01

R¹S = -6.32925+01

R¹T = -6.32925+01

R¹U = -6.32925+01

R¹V = -6.32925+01

R¹W = -6.32925+01

R¹Z = -6.32925+01

R¹A = -6.32925+01

R¹B = -6.32925+01

R¹C = -6.32925+01

R¹D = -6.32925+01

R¹E = -6.32925+01

R¹F = -6.32925+01

R¹G = -6.32925+01

R¹H = -6.32925+01

R¹I = -6.32925+01

R¹J = -6.32925+01

R¹K = -6.32925+01

R¹L = -6.32925+01

R¹M = -6.32925+01

R¹N = -6.32925+01

R¹P = -6.32925+01

R¹Q = -6.32925+01

R¹R = -6.32925+01

R¹S = -6.32925+01

R¹T = -6.32925+01

R¹U = -6.32925+01

R¹V = -6.32925+01

R¹W = -6.32925+01

R¹Z = -6.32925+01

R¹A = -6.32925+01

R¹B = -6.32925+01

R¹C = -6.32925+01

R¹D = -6.32925+01

R¹E = -6.32925+01

R¹F = -6.32925+01

R¹G = -6.32925+01

R¹H = -6.32925+01

R¹I = -6.32925+01

R¹J = -6.32925+01

R¹K = -6.32925+01

R¹L = -6.32925+01

R¹M = -6.32925+01

R¹N = -6.32925+01

R¹P = -6.32925+01

R¹Q = -6.32925+01

R¹R = -6.32925+01

R¹S = -6.32925+01

R¹T = -6.32925+01

R¹U = -6.32925+01

R¹V = -6.32925+01

R¹W = -6.32925+01

R¹Z = -6.32925+01

R¹A = -6.32925+01

R¹B = -6.32925+01

R¹C = -6.32925+01

R¹D = -6.32925+01

R¹E = -6.32925+01

R¹F = -6.32925+01

R¹G = -6.32925+01

R¹H = -6.32925+01

R¹I = -6.32925+01

R¹J = -6.32925+01

R¹K = -6.32925+01

R¹L = -6.32925+01

R¹M = -6.32925+01

R¹N = -6.32925+01

R¹P = -6.32925+01

R¹Q = -6.32925+01

R¹R = -6.32925+01

R¹S = -6.32925+01

R¹T = -6.32925+01

R¹U = -6.32925+01

R¹V = -6.32925+01

R¹W = -6.32925+01

R¹Z = -6.32925+01

R¹A = -6.32925+01

R¹B = -6.32925+01

R¹C = -6.32925+01

R¹D = -6.32925+01

R¹E = -6.32925+01

R¹F = -6.32925+01

R¹G = -6.32925+01

R¹H = -6.32925+01

R¹I = -6.32925+01

R¹J = -6.32925+01

R¹K = -6.32925+01

R¹L = -6.32925+01

4. PRACTICAL ADVICE TO THE USER

Set forth in this section are some practical guides to using the SL4 Code as deduced by the author as a result of many attempts at obtaining heating predictions.

The fundamental problem is prescribing a set of initial profiles (velocity, blown gas mass fraction, enthalpy) in a nonphysical coordinate which is sufficiently close to reality to get underway with a series of iterations. In this regard, one should start the code at stagnation point. At stagnation point, only f , C_v and H profiles need to be guessed. In Ref. 4 a detailed discussion was made on how to guess the profiles effectively at the stagnation point. Same rules should apply to the use of the SL4 Code. The term stagnation point is defined as $z = 10^{-6}$ in this code, since, when z is exactly zero, the shock layer parameters, β 's, are all undetermined.

Once the stagnation point solution is obtained, one can move a finite distance away from the stagnation point, and use the stagnation point solution as the initial guessed profiles. In this manner the user can build-up solutions around the body.. The distance one moves from point to point in obtaining the local solutions will be dependent on the shock shape and the blowing variation. In general one should move only a small distance near the stagnation region. The size of the distance between solutions, Δz , should be inversely proportional to the shock bluntness. That is, for more blunted shocks, Δz should be smaller than the value for a less blunted shock. Also, Δz is inversely proportional to the rate change of mass injection rate. The faster the injection rate changes, a smaller Δz must be chosen. From the sample calculations of Ref. 1, a rough idea of the practical value of Δz can be obtained. The symptoms which result from too large a Δz selection are, obviously, failure to obtain a convergent solution or the failure to even start the iteration process.

At what point does the heating prediction obtained by the SL4 Code constitute a "solution" to a particular entry problem? This question is at the heart of the convergence difficulties. For nonblowing problems the author has normally set a convergence level of 5% with the realization that the precision in the radiative and convective flux calculation will be at least that good. For a blowing problem the author has worked toward a goal of a 10% level of precision. By this is meant the following: Let the radiative flux at some cycle be the i^{th} value. Then, if the computation were continued an endless number of iterations, the asymptotically approached radiative heating value would be within 10% of the i^{th} value. The degree of precision is measured by comparing the radiative flux from the guessed and calculated enthalpy. The user is warned, however, that in order for the above measured precision to be valid the enthalpy profile must be converged to roughly 10% at most points across the shock layer. The exception is the few points in the shear layer region where large spatial variations occur: In the final analysis it is the responsibility of the user to interpret the results of the SL4 Code in an intelligent way.

5. REFERENCES

1. Y. S. Chou, "Radiative Coupled Viscous Flow with Massive Blowing," LMSC Rept. D311312, Nov. 1972. NASA CR-2236, 1973.
2. K. H. Wilson, "Stagnation Point Analysis of Coupled Viscous Radiating Flow with Massive Blowing," NASA CR-1548, June 1970.
3. H. Hoshizaki and L. E. Lasher, "Convective and Radiative Heat Transfer to an Ablating Body," AIAA J. Vol. 6, pp. 1441-1449, 1968.
4. K. H. Wilson, "VISC Code--A User's Manual," LMSC D31140, Oct. 1972. NASA CR-2237, 1973.

Page Intentionally Left Blank

Page Intentionally Left Blank

NATIONAL AERONAUTICS AND SPACE ADMINISTRATION
WASHINGTON, D.C. 20546

OFFICIAL BUSINESS
PENALTY FOR PRIVATE USE \$300

SPECIAL FOURTH-CLASS RATE
BOOK

POSTAGE AND FEES PAID
NATIONAL AERONAUTICS AND
SPACE ADMINISTRATION
451



POSTMASTER : If Undeliverable (Section 158
Postal Manual) Do Not Return

"The aeronautical and space activities of the United States shall be conducted so as to contribute . . . to the expansion of human knowledge of phenomena in the atmosphere and space. The Administration shall provide for the widest practicable and appropriate dissemination of information concerning its activities and the results thereof."

—NATIONAL AERONAUTICS AND SPACE ACT OF 1958

NASA SCIENTIFIC AND TECHNICAL PUBLICATIONS

TECHNICAL REPORTS: Scientific and technical information considered important, complete, and a lasting contribution to existing knowledge.

TECHNICAL NOTES: Information less broad in scope but nevertheless of importance as a contribution to existing knowledge.

TECHNICAL MEMORANDUMS: Information receiving limited distribution because of preliminary data, security classification, or other reasons. Also includes conference proceedings with either limited or unlimited distribution.

CONTRACTOR REPORTS: Scientific and technical information generated under a NASA contract or grant and considered an important contribution to existing knowledge.

TECHNICAL TRANSLATIONS: Information published in a foreign language considered to merit NASA distribution in English.

SPECIAL PUBLICATIONS: Information derived from or of value to NASA activities. Publications include final reports of major projects, monographs, data compilations, handbooks, sourcebooks, and special bibliographies.

TECHNOLOGY UTILIZATION PUBLICATIONS: Information on technology used by NASA that may be of particular interest in commercial and other non-aerospace applications. Publications include Tech Briefs, Technology Utilization Reports and Technology Surveys.

Details on the availability of these publications may be obtained from:

SCIENTIFIC AND TECHNICAL INFORMATION OFFICE

NATIONAL AERONAUTICS AND SPACE ADMINISTRATION

Washington, D.C. 20546